Ultrahigh-Performance Concrete Segmental Bridge Technology: Toward Sustainable Bridge Construction

Yen Lei Voo[1]; Stephen J. Foster[2]; and Chen Cheong Voo[3]

Abstract: This paper presents the current state of practice in the development of ultrahigh-performance concrete (UHPC) bridge construction in Malaysia. Since 2006, Dura Technology (DT) has pioneered research in the optimal uses of UHPC in bridge construction through its Sustainable Bridge Construction Initiative. After several years of research and development work, DT has collaborated with the Malaysia Works Ministry to design and build bridges in some of their bridge projects, especially those bridges under the rural development program where sourcing of material, site access, and construction method are major challenges when using conventional methods. The most current information and details on the completed and ongoing UHPC bridge projects in Malaysia are presented. To date, a total of 26 segmental UHPC bridge projects have been constructed and opened for service. In this paper, a selected UHPC bridge case study is examined in terms of the design aspects, quality control, constructability, and of how UHPC has helped to make the bridge more affordable, sustainable, easier to build, and economical. **DOI: 10.1061/(ASCE)BE.1943-5592.0000704.** © *2014 American Society of Civil Engineers.*

Author keywords: Ultrahigh performance; Ductile; Fiber; Segmental; Bridge; Sustainable.

Downloaded from ascelibrary.org by Southeast University on 11/21/22. Copyright ASCE. For personal use only; all rights reserved.

Introduction

Ultrahigh-performance concrete (UHPC) is an advanced cementitious-based composite material that offers new opportunities for current or future infrastructure development in both urban-suburban regions and rural areas. UHPC in its present form has become commercially available in many countries, such as Australia and New Zealand (Rebentrost and Wight 2011), Austria (Freytag et al. 2012), Canada (Blais and Couture 1999), Germany (Schmidt 2012), Italy (Meda and Rosati 2003), Japan [Japan Society of Civil Engineers (JSCE) 2006], Malaysia (Voo et al. 2011), Netherlands (Kaptijn and Blom 2004), Slovenia (Šajna et al. 2012), South Korea (Ricciotti 2002), the United States (Graybeal 2011), and other countries. A complete search of the literature has identified more than 100 completed bridges (pedestrian and motorway bridges combined) constructed using UHPC in one or more components. Both private and governmental bodies are directing increasing attention and initiative toward exploiting UHPC as the future construction material, in the belief that UHPC technology embraces the complete solution for sustainable constructions (Ng et al. 2012; Voo and Foster 2010).

[1]Chief Executive Officer and Director, Dura Technology, Lot 304993, Jalan Chepor 11/8, Pusat Seramik Fasa 2, Ulu Chepor, 31200, Chemor, Perak, Malaysia; Adjunct Professor, Civil Engineering Dept., Univ. Putra Malaysia (UPM), Serdang, 43400, Malaysia (corresponding author). E-mail: vooyenlei@dura.com.my

[2]Professor, Head of School, Civil and Environmental Engineering, Univ. of New South Wales Australia, Sydney NSW 2052, Australia. E-mail: s.foster@unsw.edu.au

[3]Project Manager, Dura Technology, Lot 304993, Jalan Chepor 11/8, Pusat Seramik Fasa 2, Ulu Chepor, 31200, Chemor, Perak, Malaysia. E-mail: gregoryvoo@dura.com.my

Note. This manuscript was submitted on January 10, 2014; approved on September 9, 2014; published online on October 3, 2014. Discussion period open until March 3, 2015; separate discussions must be submitted for individual papers. This paper is part of the ***Journal of Bridge Engineering***, © ASCE, ISSN 1084-0702/B5014001(12)/$25.00.

In Germany, one of the major initiatives has been the 12 million Euro research program funded by the German Research Foundation and awarded in 2005, which involved 34 research projects at more than 20 research institutes in Germany (Schmidt 2012). The purpose of the program was to expand the basic knowledge so that reliable technical standards could be developed. The goal was to make UHPC a reliable, commonly available, economically feasible, and regularly applied material. Another example of a major research initiative in the use of UHPC is the Korean Institute of Construction Technology (KICT) US$11 million Super 200 program that has been studying the use of UHPC in cable-stayed bridges since 2007 (Kim et al. 2012).

It is reported that the U.S. Federal Highway Administration (FHWA) began investigating the use of UHPC in 2001, with the first structure, the 33-m Mars Hill Road bridge in Iowa, constructed in 2006 (Graybeal 2011). Since this time, a few more bridges have been constructed (including Virginia's Cat Point bridge and Iowa's Jakway Park bridge, both in 2008); however, the technology is used mostly as a jointing material between adjacent precast girders, or deck panels, constructed of conventional technologies.

The first structure to use UHPC in its construction was the 60-m single-span Sherbrooke pedestrian bridge crossing the river of Magog, Province of Quebec, Canada (Lachemi et al. 1998). The walkway deck, which serves as the top chord to the truss, consists of 3.3-m-wide by 30-mm-thick UHPC slabs. The web members are of a composite design involving UHPC placed in thin-walled stainless steel tubing. The success of this structure dawned a new era in design methodology of concrete structures.

The first major structures adopting UHPC technology were footbridges. In April 2002, the Seonyu footbridge (the Footbridge of Peace) in Seoul, South Korea, was constructed using UHPC (Behloul and Lee 2003). The structure connects the city of Seoul to Seonyu Island on the Han River. Constructed by Bouygues Construction, the bridge consists of an arch with a 120-m span supporting a 30-mm-thick UHPC deck. The structure required only about half of the amount of material that would have been used with traditional concrete construction, yet provides equivalent load-bearing and strength properties. Around the same time as the construction of the Seonyu bridge was the 50-m footbridge

Downloaded from ascelibrary.org by Southeast University on 11/21/22. Copyright ASCE. For personal use only; all rights reserved.

constructed in Sakata (Sakata-Mirai footbridge), which is located in the northwestern region of the island of Honshu, Japan (Tanaka et al. 2011). Indeed, the Japanese were among the first to apply UHPC in the design and construction of segmental footbridges, with other examples including the 36.4-m-span Akakura Onsen Yukemuri bridge (completed in 2004), the 64.5-m-span Hikita footbridge (completed in 2007), the 81.2-m-span Mikaneike footbridge (completed in 2007), as well as many others (Tanaka et al. 2011; Musha et al. 2013). Since the construction of the Seonyu and Sakata-Mirai footbridges, UHPC bridges for pedestrian traffic have been constructed in France, New Zealand, Spain, Germany, and elsewhere (Toutlemonde and Resplendino 2011).

The first road bridges to be constructed using UHPC technology appeared in 2005, with four bridges constructed at around the same time. One of these is the 16-m-span, 21-m-wide Shepherd's Gully bridge located 150 km north of Sydney, Australia, and constructed by VSL; it is a precast, pretensioned, I-girder bridge (Foster 2009; Rebentrost and Wight 2011). Two bridges were constructed in France in 2005: (1) the n34 overpass of the A51 (PS34) motorway, and (2) the Saint Pierre La Cour bridge (Resplendino 2008). The PS34 bridge is of single-span, 47.4-m-long, prestressed segmental box girder construction, with 22 UHPC box segments, and the Saint Pierre La Cour bridge is of precast, prestressed I-girder construction with a composite deck. The last of the four is the 16.6-m Horikoshi C-ramp bridge in Japan (Tanaka et al. 2011). In all cases, the girders do not have any conventional reinforcement for shear or bursting stresses but are reinforced longitudinally with tendons.

In 2007, Tokyo Monorail with Taisei Corporation constructed a 40-m-long monorail girder of UHPC (Tanaka et al. 2011). The girder was constructed in three segments and joined together on site by a combination of wet and dry joints. The monorail girder was reportedly the longest UHPC simple-span bridge member at the time of construction.

In 2008, the world's first segmental UHPC composite deck road bridge was constructed; a single-span, 46.0-m ground support equipment (GSE) bridge was built over a road connecting the south and north apron in the extension of the Tokyo International Airport project. At the time, the road bridge was the largest UHPC road bridge in the world (Tanaka et al. 2011).

The significance of such technology lies not only in the great enhancements in concrete strengths, leading to lighter-weight construction and more efficiency of materials, but also in the contribution of UHPC to sustainability through lower carbon footprints (Voo and Foster 2010). This aspect is addressed in this paper and an example is presented.

Since 2006, Dura Technology (DT) in Malaysia has pioneered research in the optimal uses of UHPC in bridge construction through its Sustainable Bridge Construction Initiative. During several years of research and development, DT has been collaborating with the Malaysia Works Ministry to design and build bridges in some of their bridge projects, especially those bridges under the rural development program where sourcing of material, site access, and construction method are major challenges when using conventional methods. In all, a total of 36 bridges either have been constructed or are under construction by DT using UHPC technology. Of these bridges, 26 are segmental construction, and 10 are pretensioned girders having spans of less than 22 m. Table 1 provides a list of the 26 completed and ongoing segmental bridge projects that DT has been involved with in Malaysia.

Fig. 1 shows examples of the two types of segmental bridge construction adopted in Malaysia: (1) UHPC U-girders with composite deck, and (2) stitched T-girder construction. Among the 26 UHPC segmental bridge projects, 20 bridges have been completed and are open to traffic; six are due for completion in 2014.

When completed in January of 2011, the 50-m, single-span Kampung-Linsum bridge was the world's longest composite box deck bridge in which the main girders were constructed of UHPC (Voo et al. 2011). Since that time, similar construction technology was used for the 51.6-m-span Rantau-Siliau and 52-m Sungai-Ara bridges (both completed in 2013). These will be surpassed by the 100-m-span Batu bridge when it is completed in November 2014.

In this paper, a selected UHPC bridge project, the three-span Sungai Nerok bridge (No. 13 in Table 1), is described in terms of its design aspects, quality control, and constructability; the paper also explains how a UHPC bridge is more economical, sustainable, and easier to build in less accessible regions. In many circumstances, a UHPC bridge construction is able to realize the following advantages: (1) immediate and life-cycle cost savings; (2) enhancement in design/service life of structures; (3) low maintenance of the UHPC components due to their good durability; (4) reduced overall construction time and risk; (5) reduced consumption of raw materials, thereby representing a more ecofriendly choice; (6) lighter superstructure dead weight permitting lighter/smaller substructure/foundations; (7) reduced manpower and smaller machinery required; (8) better quality than in situ wet work and precast high-performance concrete structures; and (9) less environmental impact on the construction site due to shorter-duration temporary work.

UHPC

The steel fiber-reinforced UHPC used in the beams in all bridges given in Table 1 is Grade 150 ductile concrete supplied by DT. The material used to produce UHPC consists of the following: Type I ordinary portland cement; densified silica fume, which contains more than 92% silica dioxide (SiO_2) and has a surface fineness of 23,700 m^2/kg; and washed-sieved fine sand, with a particle size range between 100 and 1,000 μm. The superplasticizer used was polycarboxylic ether (PCE)-based superplasticizer. Two types of steel fibers were used; both were manufactured from 2,500 MPa high-carbon steel wire. Type 1 steel fiber was of straight shape (SS) and was supplied with dimensions 20-mm length by 0.2-mm diameter. Type 2 steel fiber was end-hooked (EH) and had dimensions of 25-mm length by 0.3-mm diameter. One percent of each fiber type was used for a total of 2% by volume. A benchmark value for the specification of the UHPC has been set by DT, which is a mean 28-day cube compressive strength and 28-day flexure strength not less than 150 and 20 MPa, respectively.

Shear Keys

The strength and serviceability behavior of a segmental bridge depends very much on the performance of its joints. Early segmental bridges typically adopted a single key in the web section and, often, these were reinforced. Contemporary practice, however, is to use multiple unreinforced keys that are distributed through the depth and width of the connection (Zhou et al. 2005). A review of the literature on practices and testing was given in Li et al. (2013a, b), Saibabu et al. (2013), and Buyukozturk et al. (1990). Although considerable testing has been undertaken to investigate the behavior of conventional precast segmental decks with external tendons and dry joints, no research has been conducted on shear connections of UHPC joints. Before the 50-m-span Kampung Linsum bridge (No. 1 in Table 1) could be certified by the Malaysian Public Works Department, an experimental study needed to be conducted on full-scale joint key models with a geometry closely resembling the key

J. Bridge Eng., 2015, 20(8): B5014001

Downloaded from ascelibrary.org by Southeast University on 11/21/22. Copyright ASCE. For personal use only; all rights reserved.

Table 1. Summary of the Application of UHPC Segmental Bridges in Malaysia

Number	Year	Bridge	Location	Span	Segment length/total length (m)	Total width (m)	Application	Live load	Type[a]	Beam shape	Status
1	2010	Kg. Linsum	Rantau, Negeri Sembilan	1	5 + 8 + 8 + 8 + 8 + 8 + 5/50	4.8	Medium traffic	HA or 30 HB	2	U	Completed
2	2011	Ulu Geroh	Gopeng, Perak	1	5 + 5 + 5 + 5 + 5/25	3.5	Medium traffic	HA or 30 HB	1	T	Completed
3		Ulu Kampar	Gopeng, Perak	1	6 + 6 + 6/18	3.5	Medium traffic	HA or 30 HB	1	T	Completed
4		Ulu Kinta	Ipoh, Perak	1	15.75 + 15.75/31.5	3.5	Medium traffic	HA or 30 HB	1	T	Completed
5		Kg. Beng	Lenggong, Perak	1	6 + 6/12	3.5	Medium traffic	HA or 30 HB	1	T	Completed
6		Ulu Chemor	Chemor, Perak	1	14.5 + 14.5/29.5	3.5	Medium traffic	HA or 30 HB	1	T	Completed
7		School Taayah	Ipoh, Perak	1	15 + 10 + 15/40	2.5	Pedestrian	5 kPa	1	T	Completed
8	2013	Titi	Jelebu, Negeri Sembilan	1	5 + 8 + 8 + 8 + 8 + 8 + 5/50	11.9	Highway	HA or 45 HB	2	U	Completed
9		Kg. Bermin	Tapah, Perak	1	5 + 8 + 8 + 8 + 8 + 5/42	3.5	Medium traffic	HA or 30 HB	2	U	Completed
10		Kg. Malau	Lawin, Perak	1	15 + 15/30	3.5	Medium traffic	HA or 30 HB	1	T	Completed
11		Rantau-Siliau	Rantau, Negeri Sembilan	1	5.8 + 8 + 8 + 8 + 8 + 8 + 5.8/51.6	18.3	Highway	HA or 45 HB	2	U	Completed
12		Kuala Sepetang	Taiping, Perak	5	11 + 11/22	3.8	Pedestrian/motorcycle	5 kPa	1	U	Completed
13		Sg. Nerok	Lenggong, Perak	3	15 + 15/30	15	Highway	HA or 45 HB	1	T	Completed
14		Kg. Chuar	Kati, Perak	1	15 + 15/30	11.7	Highway	HA or 45 HB	1	T	Completed
15		Sg. Ara	Kerian, Perak	1	6 + 8 + 8 + 8 + 8 + 8 + 6/52	5	Medium traffic	HA or 30 HB	2	U	Completed
16		Sg. Kurau 1	Kerian, Perak	1	5 + 8 + 8 + 8 + 8 + 8 + 5/50	5	Medium traffic	HA or 30 HB	2	U	Completed
17		Sg. Kurau 2	Kerian, Perak	1	5 + 8 + 8 + 8 + 8 + 8 + 5/50	5	Medium traffic	HA or 30 HB	2	U	Completed
18		Mardi	K. Kangsar, Perak	1	16 + 16/32	8	Medium traffic	HA or 30 HB	1	T	Completed
19	2014	Kg. Dato Banir	Batang Padang, Perak	1	14.5 + 14.5/29	13.9	Highway	HA or 45 HB	2	T	Ongoing
20		Sg. Choh	Ipoh, Perak	1	4 + 8 + 8 + 8 + 4/32	22	Highway	HA or 45 HB	2	U	Completed
21		Wisma LKIM	Puchong, Selangor	1	16 + 16/32	22.1	Highway	HA or 45 HB	1	T	Completed
22		Kg. Baharu- Kg. Teluk	Manjung, Perak	10	4.75 + 8 + 8 + 8 + 8 + 4.75/41.5	13.9	Highway	HA or 45 HB	2	U	Ongoing
23		Batu 6	Gerik, Perak	1	2.5 × 40 pieces/100	5	Medium traffic	HA or 30 HB	1	Box	Ongoing
24		Sg. Yap	Jerantut, Pahang	1	4.75 + 8 + 8 + 8 + 8 + 8 + 4.75/49.5	5	Medium traffic	HA or 30 HB	2	U	Ongoing
25		Kg. Merdeka	Teluk Intan, Perak	1	4.75 + 8 + 8 + 8 + 8 + 8 + 8 + 4.75/57.5	5	Medium traffic	HA or 30 HB	2	U	Ongoing
26		Central Forest Spine	Gerik, Perak	5	3.75 + 8 + 8 + 8 + 8 + 3.75/39.5	17.4	Highway	HA or 45 HB	2	U	Ongoing

Note: Kg. = Kampung, which means *village*; Sg. = Sungai, which means *river*.

[a]Type 1 = UHPC integral beam deck system; type 2 = UHPC beam composited with in situ deck.

Downloaded from ascelibrary.org by Southeast University on 11/21/22. Copyright ASCE. For personal use only; all rights reserved.

Fig. 1. Examples of UHPC segmental bridge construction (images by Yen Lei Voo): (a–d) 51.6-m-span Rantau-Siliau bridge, U-shaped UHPC girder with composite conventional strength concrete deck; (e and f) 30-m-span Ulu Chemor bridge, stitched T-girder construction

joint of actual bridge girder segments. Six dry-keyed joints were manufactured from UHPC and were tested; the experimental parameters were the number of shear keys and the confining stress.

The female joint specimens were poured first with all specimens cast vertically in steel forms and were compacted using a vibrating table. Within 30 min of casting, the exposed surface of the specimens and test control samples were sprayed with a curing compound. After 24 h, the male joint section was matched cast against the female component using a similar procedure to the female element. The full specimens were stripped at the age of 3 days from the casting of the female element, and the shear joint specimens, and the control specimens, then were cured for 48 h more at 90°C in a hot-water tank. At the age of 5 days, all the specimens were removed from the hot-water tank and air cured until the day of testing.

Specimens Experimental Setup and Test Procedure

The shear joint test was undertaken using a push-off setup arrangement, similar to that used by Buyukozturk et al. (1990), with the test setup used enabling shear to be applied across the shear plane with negligible moment. Details of the specimens and the test arrangements are given in Fig. 2. The specimens are designated as SKN_k-σ_n. For example, Specimen SK5-10 indicates the specimen had five shear keys and an applied confining pressure of 10 MPa. All specimens were 200 mm thick. The confining stress was applied to the joint surfaces through a stiff steel framework and loaded using 15.2-mm-diameter prestressing strands. Two confining pressures were applied (10 and 20 MPa). For the specimens with 10 MPa of confinement, a total of eight strands were used with each strand stressed to 200 kN using a hydraulic monojack and then anchored. Similarly, 16 strands were used for the specimens with a confining stress of 20 MPa. Each strand was tensioned at least three times to minimize the loss of stress.

Each specimen was loaded at the centerline of the shear plane (Fig. 2) and slip measured using LVDTs. The load was applied to the load-bearing supports via a layer of hard rubber sandwiched by a 50-mm-thick high-strength steel plate. Each half of the specimens was separated by a 50-mm gap at their loading heads so that the applied force was resisted solely by shear through the line of the keys.

Material and Geometric Properties

The mean compressive strength of the concrete (f_{cm}) was determined from six 150-mm-high by 75-mm-diameter cylinders with their ends ground flat; the results are given in Table 2. The modulus of elasticity determined from the average of six 200-m-high by 100-mm-diameter cylinders was $E_c = 46$ GPa. The flexural tensile properties of the material were determined from three-point flexure bending tests undertaken in accordance with the recommendations of RILEM TC 162-TDF (RILEM 2002). Two representative values of the residual flexural tensile strengths were measured, $f_{R,\delta=0.47\text{mm}}$ and $f_{R,\delta=2.07\text{mm}}$, corresponding to the strengths measured at midspan displacements

J. Bridge Eng., 2015, 20(8): B5014001

Downloaded from ascelibrary.org by Southeast University on 11/21/22. Copyright ASCE. For personal use only; all rights reserved.

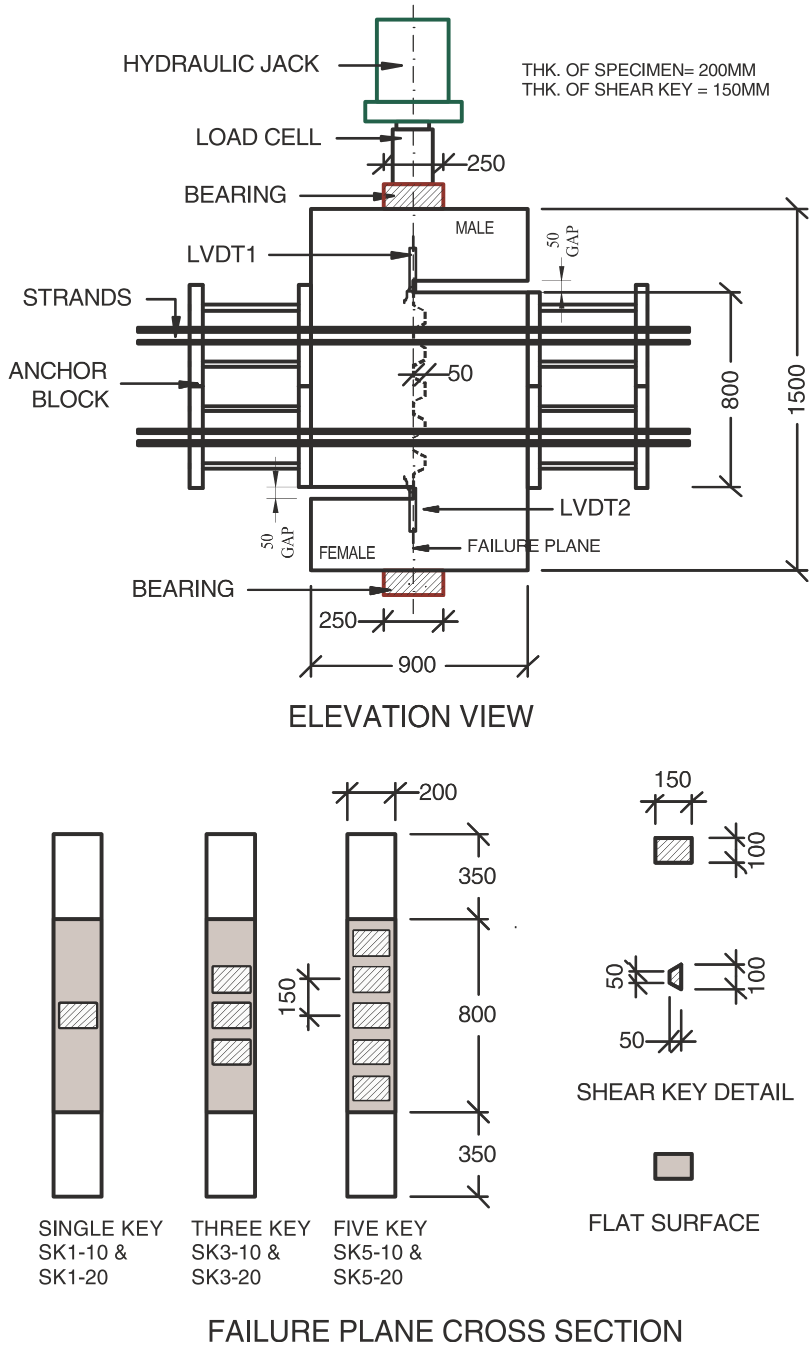

Fig. 2. Transducer arrangement and typical experimental setup (dimensions in millimeters)

Table 2. Experimental Arrangements and Test Results

Specimen	f_{cm} (MPa)	$f_{sp,u}$ (MPa)	A_k (mm^2)	A_{sm} (mm^2)	$V_{j,cr}$ (kN)	$V_{j,u}$ (kN)	$V_{j,\text{friction}}$ (kN)	$\mu = \frac{V_{j,\text{friction}}}{P_i}$	$\tau_{j,cr}$ (MPa)	$\tau_{j,u}$ (MPa)
SK5-10	148	14.5	75×10^3	85×10^3	1,470	2,174	750	0.47	9.19	13.6
SK5-20	148	14.5	75×10^3	85×10^3	1,770	2,394	1,148	0.36	11.06	15.0
SK3-10	148	14.0	45×10^3	115×10^3	1,090	1,516	738	0.46	6.81	9.48
SK3-20	148	14.0	45×10^3	115×10^3	1,500	2,014	1,144	0.36	9.38	12.59
SK1-10	149	14.9	15×10^3	145×10^3	911	1,110	720	0.45	5.69	6.94
SK1-20	149	14.9	15×10^3	145×10^3	1,262	1,545	1,120	0.35	7.89	9.66

Downloaded from ascelibrary.org by Southeast University on 11/21/22. Copyright ASCE. For personal use only; all rights reserved.

of 0.47 and 2.07 mm, respectively. The modulus of rupture was obtained from the testing of three 100-mm-square prisms with a notch depth of 30 mm and determined as $f_{cf} = 35$ MPa; the residual tensile strengths were $f_{R,\delta=0.47\mathrm{mm}} = 29$ MPa and $f_{R,\delta=2.07\mathrm{mm}} = 31$ MPa.

According to JSCE (2006), the cracking strength ($f_{sp,cr}$) of the UHPC can be determined using split-cylinder tests with an electronic transducer attached to the specimens at 90° to the direction of the applied load. Using this method, the tensile strength was determined, from 200-mm-long by 100-mm-diameter cylinders, to be $f_{sp,cr} = 8$ MPa. After cracking, the UHPC cylinders continued to resist higher tensile stresses until peak strength was attained. The tensile strengths ($f_{sp,u}$) are given in Table 2.

In Table 2, A_k is the total area for all keys across the shear plane, measured at their base, and, A_{sm} is the area of the smooth section of the joint. The sum of A_k and A_{sm} gives the total area of the section in shear.

Test Results and Observations

The experimental results are summarized in Table 2, in which $V_{j,cr}$ is the point on the force displacement history graph where nonlinearity was first observed, indicating first damage of the keys; $V_{j,u}$ is the maximum load carried by the joint; $V_{j,\mathrm{friction}}$ is the residual frictional shear force after failure; and P_i is the initially applied normal force across the joint. The average shear strength (τ) is defined as the maximum load divided by the total projected area of the joint, or shear plane, and is equal to $A_{\mathrm{joint}} = 800 \times 200 = 160 \times 10^3$ mm^2, where $\tau_{j,cr}$ is taken at the point of cracking and $\tau_{j,u}$ is at ultimate.

The slips between the surfaces were minimal until the peak load was achieved. After the peak load was reached, the keys slid and a sudden drop in load was observed. In all cases, failure was initiated at the base of the bottom keys of the male component.

Fig. 3(a) shows the female component before testing and Fig. 3(b) shows a typical failure through the keys of the male component. After the shear key had cracked, the strength was derived from the steel fibers crossing the shear plane. When the maximum vertical shear resistance of the joint was reached, the applied confining pressure provided a frictional resistance to keep the two halves of the specimen from separating. The results show that the shear strength increased with the increase in confining stress and with an increasing number of shear keys. In addition, the test results showed that the higher the confinement stress, the slower the separation of the shear key from the joint, accompanied by a decrease in the friction coefficient. It is postulated that the decrease in the friction for the higher confinement tests was owing to a surface polishing effect that may occur with the higher applied normal force (P_i).

After the peak load was attained, the specimens were unloaded to zero and reloaded to their frictional capacity. The average coefficients of friction were measured to be $\mu = 0.46$ and $\mu = 0.36$ for the 10 and 20 MPa confinement series, respectively. The shear force versus displacement measured for Specimen SK3-10 is shown in Fig. 4 and is typical of the observed behavior.

Proposed Model for UHPC-Keyed Joints

Numerous design models are available in the literature for the calculation of the shear strength of unreinforced concrete shear-keyed connections; however, no models exist for UHPC-keyed joints. It has been demonstrated that, for members subjected to beam shear, steel fiber-reinforced UHPC provides sufficient ductility so as to allow for design by plasticity methods (Voo et al. 2006, 2010). In the proposed model, steel fiber-reinforced UHPC was treated as a plastic material. The shear strength and minor principal (tensile) stress can be obtained by the principle of Mohr's circle as

$$\sigma_1 = \frac{\sigma_x + \sigma_y}{2} + \sqrt{\left(\frac{\sigma_x + \sigma_y}{2}\right)^2 + \tau_{xy}^2} \tag{1}$$

where σ_1 = major principal (tensile) stress; σ_x and σ_y = normal stresses in the x- and y-directions, respectively; and τ_{xy} = shear stress. In this case $\sigma_x = \sigma_n$ (taking compression as positive), $\sigma_y = 0$, and, for limit states design, one substitutes $\sigma_1 = f_t$, where f_t = uniaxial tensile strength of the composite. The shear stress then can be determined from

$$\tau_{xy} = \sqrt{\left(f_t + \frac{\sigma_n}{2}\right)^2 - \left(\frac{\sigma_n}{2}\right)^2} \tag{2}$$

The shear capacity of the joint (V_j) is calculated as the sum of the frictional component of the contact surfaces (V_{sm}) and the shear strength contribution of the keys (V_k)

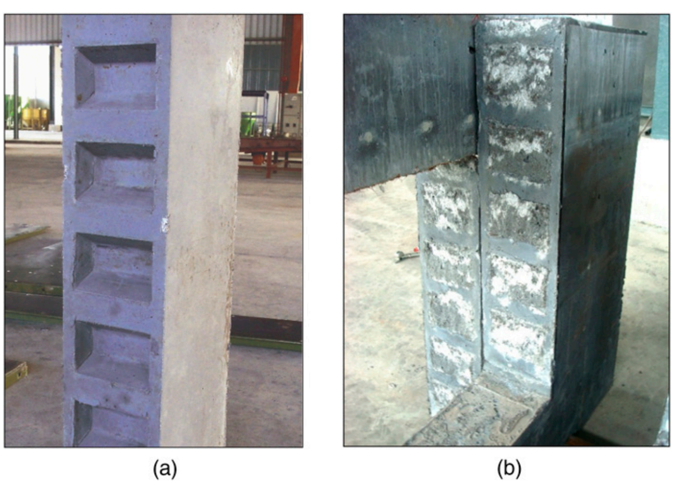

Fig. 3. (a) Female component of the joint before testing; (b) Specimen SK5-20 after testing (images by Yen Lei Voo)

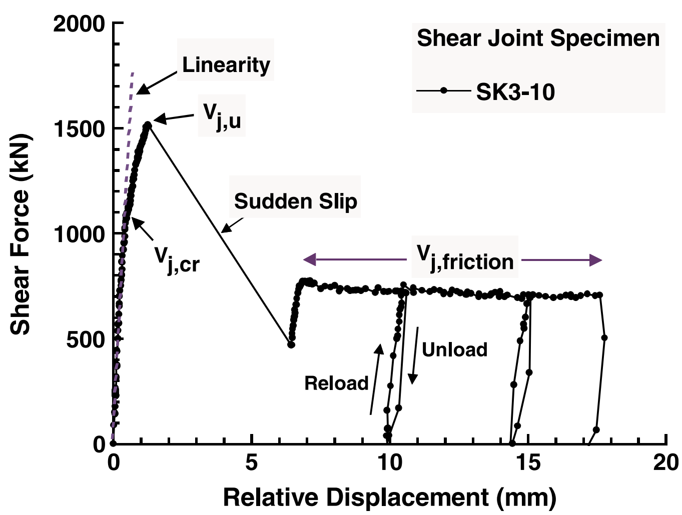

Fig. 4. Example on shear force versus relative displacement for Specimen SK3-10

J. Bridge Eng., 2015, 20(8): B5014001

$$V_j = V_{sm} + V_k \quad (3)$$

The frictional force due to the normal stress is

$$V_{sm} = \mu A_{sm} \sigma_n \quad (4)$$

where A_{sm} = area of the smooth section of the joint; σ_n = average normal pressure across the joint; and μ = static coefficient of friction. The shear strength of the keys is calculated as

$$V_k = \sum_{i=1}^{n} A_{ki} \tau_{xy} \quad (5)$$

where A_{ki} = area of shear key i; and n = number of keys.

The shear joint capacity is determined from Eqs. (1)–(5) and the results of the model are compared with test data in Table 3. The minor principal strength at ultimate is taken as $f_t = 0.9 f_{sp,u}$. It is seen that the model compares reasonably with the test data with a mean experimental/model ratio of 1.17 and coefficient of variation (COV) of 0.053. More test data are needed to validate the accuracy of the approach for a wider range of normal stresses and to determine the frictional resistance for applied normal stresses outside of the range tested in this study.

Case Study: Sungai Nerok Bridge

In 2012, the Malaysian Public Works Department tendered a road bridge project at Sungai Nerok, Lenggong of Perak state. This multispan, continuous road bridge was designed to withstand full highway loading, per specification BD 37/01 (Highways Agency 2001), and comprises a total width of 15 m and three spans of 30 m each, creating a total bridge length of 90 m. The completed bridge is shown in Fig. 5(a) and the span arrangement in Fig. 5(b).

The superstructure of the bridge was constructed using a posttensioned segmental UHPC integral beam-deck system, which was fully integral with the substructure/foundation. The foundation of the bridge was seated on 600-mm-diameter Grade 80 MPa spun piles driven to set at an approximate pile length of 36 m. Fig. 5(b) shows the typical cross section of the UHPC bridge. The UHPC beams were spaced 1.5 m center to center and each span consists of 10 beams. A total of 30 beams were used. Unlike conventional bridge designs, the UHPC bridge does not require in situ concrete decking, and the UHPC girders do not have any shear reinforcement in their thin web.

Fig. 6 shows the details of a typical UHPC precast beam. Each beam was delivered to site in pairs of 15-m-long segments. After posttensioning, the beam had a total length of 30 m. The top flange of the beam was 1.2 m wide (before stitching/jointing) and consisted of four 15.2-mm-diameter strands; the bottom flange was 400 mm wide and consisted of 19 15.2-mm-diameter strands. The strands used were of seven-wire low-relaxation type with a specified breaking load of 260 kN per strand. The web was designed as a thin membrane of 100 mm in thickness.

Quality Control and Inspection Plan

Very strict quality control and inspection plans were implemented during the production of the UHPC segments/beams. Each beam consisted of two segments, jointed using posttensioning with the segmental joint at the beam midspan. A total of 60 segments were produced over a period of 3 months. Each segment was produced with a new batch of concrete mixing; therefore, control samples were collected for every batch of the concrete mix. A total of 60 sets of samples were collected (i.e., a minimum of nine 100-mm cubes and a minimum of three prisms).

Fig. 7 presents the statistical distribution of the strength test results for the quality control specimens. The cube compressive strength f_{cu} was measured using three cube specimens. The early-age (1-day) and 28-day strengths were measured and are presented. In general, the UHPC was able to achieve 1- and 28-day characteristic compressive strengths of $f_{ck,1d} = 68$ MPa and $f_{ck,28d} = 153$ MPa, respectively, and achieved a characteristic ultimate flexural strength of $f_{cfk} = 23$ MPa. Therefore, the strength test results satisfied the benchmark requirements of DT.

In addition to the quality control measures applied for the batching processes, the following quality measures were used within the factory to ensure good fiber distributions and sectional capacities: (1) the casting temperature of the fresh concrete was controlled, with curing at 90°C and 100% humidity for a period of 48 h within 3 days after stripping of the formwork; and (2) full-scale testing was performed for shear and flexure to satisfy third-party evaluators.

Design Actions, Design Resistance, and Destructive Performance Load Test

Sungai Nerok bridge was designed to withstand the worst possible load case results from the combined action of the HA + KEL loadings and 45 U HB traffic loadings, per the requirements of BD 37/01. The "Design Actions" column in Table 4 summarizes the calculated maximum design shear force effect (V_{Ed}) and design moment effect (M_{Ed}) that may occur in a single UHPC beam under the limit state design; V_{ser} and M_{ser} are shear force and bending moment, respectively, at service conditions. In terms of structural capacity, the design shear force resistance (V_{Rd}) and design moment resistance (M_{Rd}) were calculated based on the recommendation of JSCE Guidelines for Concrete No. 9 (JSCE 2006) and are presented in the "Resistance (Factored)" column of Table 4. The material factor (γ) used in the calculation was $0.85/1.3$ for UHPC and $1/1.15$ for strands and steel reinforcement. Knowing that UHPC is a new material without a confirmed design code, the Malaysia Works Ministry required a demonstration of the structural performance of the UHPC beam relative to the computed design load actions and

Table 3. Comparison of the Proposed Shear Joint Model with the Experimental Data

Specimen	Friction		Shear key			Shear strength, $V_{j,u}$		
	μ	V_{sm} (kN)	σ_{11} (MPa)	τ_{xy} (MPa)	V_k (kN)	Experimental (kN)	Model (kN)	Experiemental/Model
SK5-10	0.46	391	13.05	17.3	1,301	2,174	1,692	1.28
SK5-20	0.36	612	13.05	20.8	1,558	2,394	2,170	1.10
SK3-10	0.46	529	12.60	16.9	759	1,516	1,288	1.18
SK3-20	0.36	828	12.60	20.3	912	2,014	1,740	1.16
SK1-10	0.46	667	13.41	17.7	266	1,110	933	1.19
SK1-20	0.36	1,044	13.41	21.2	318	1,545	1,362	1.13

J. Bridge Eng., 2015, 20(8): B5014001

Downloaded from ascelibrary.org by Southeast University on 11/21/22. Copyright ASCE. For personal use only; all rights reserved.

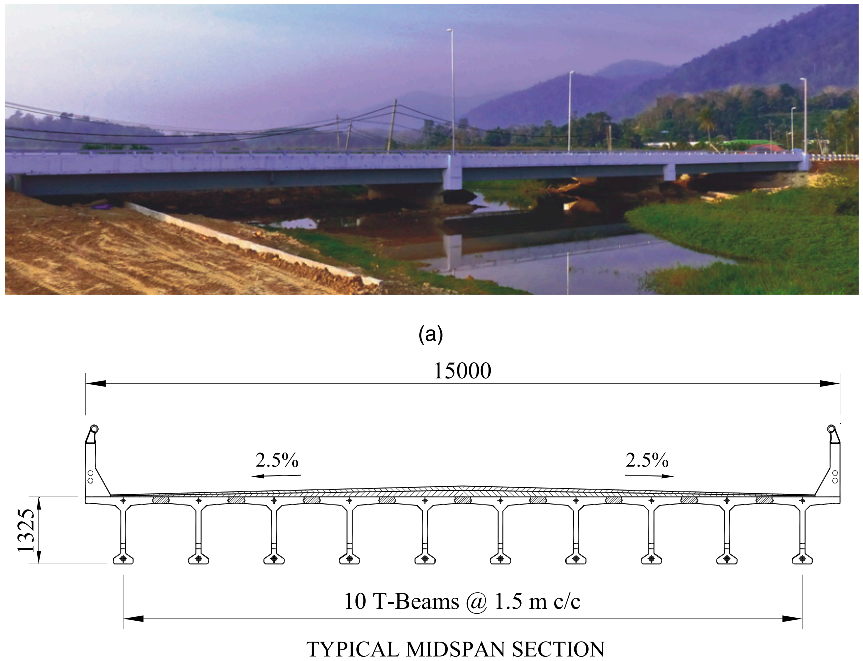

(a)

(b)

Fig. 5. (a) Sungai Nerok bridge (image by Yen Lei Voo); (b) typical section view

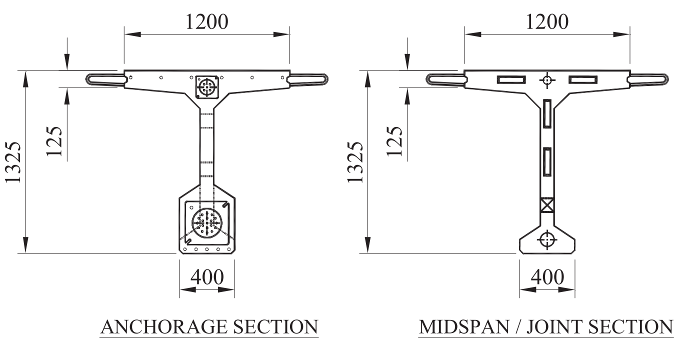

Fig. 6. Typical cross-sectional details of a segmental UHPC T-bridge girder

resistances. To this end, DT conducted full-scale destructive tests on the proposed UHPC beam.

Fig. 8(a) shows the test setup on a 30-m-long UHPC posttensioned beam in a flexural strength test. The flexure beam was tested in four-point load configurations and simply supported over a supporting length of the 26-m span. A 5,000-kN capacity hydraulic jack was placed at the center of a spreader beam and then distributed onto the top flange of the beam. One end of the beam was a pinned support whereas the other end was sitting on a pin and roller support. The pins and roller were greased to minimize friction and give free rotation and horizontal translation, as required. Nine sets of LVDTs were used to capture the vertical displacement of the beam. A total of 198 sets of demountable mechanical (DEMEC) strain gauges were used to capture the compressive strains at the top flange, tension strain/crack width at the bottom flange, and opening displacement of the segmental joint. The beam was tested until it broke into two separated segments at the midspan (i.e., where the segmental joints located). After the flexure test, an undamaged segment of the beam was configured for the shear strength test. The shear beam was tested in three-point load configurations and simply supported over a supporting length of 11-m span. The shear span-to-effective depth ratio (a/d_e) was 3. Similar to the flexure test, one end of the beam was a pinned support whereas the other end was sitting on a pin and roller support. Seven sets of LVDTs were used to capture the vertical displacement of the beam and a total of 57 sets of DEMEC gauges were used to capture the strain rosettes of the web under shear. The full experimental details and results were documented by Ikram QA Services (2011) and Voo et al. (2011).

The Experimental Results column in Table 4 presents the maximum experimental loads of the tests, where $V_{u,\exp}$ and $M_{u,\exp}$ are the measured experimental maximum shear capacity and ultimate moment capacity of the UHPC beam, respectively. In the flexure strength test, prior to failure, the segmental joint opened first, and, subsequently, more flexure cracks formed with the cracks uniformly distributed across the span as the applied load increased. Results showed that, at the applied load of $P_{u,\exp} = 800$ kN (i.e., 89% of the ultimate failure load), a large number of flexural microcracks appeared across the bottom flange/web area with measured crack widths of 0.02 to 0.06 mm in the monotonic section, whereas in the segmental joint section, a maximum opening of 4 mm was measured. The tested UHPC beam, therefore, was proven to be stronger than the design moment effects in both service limit state (SLS) and ultimate limit state (ULS) conditions. The maximum applied load captured was $P_{u,\exp} = 900$ kN, which corresponds to a maximum applied moment of $M = 900/2 \times (26/2 - 1) = 5{,}400\ \mathrm{kN \cdot m}$ at the midspan. It was concluded that the UHPC beam had ample reserve sagging moment resistance against the design positive moment effect, achieving a safety factor of 2.2 over the design service load.

In the shear strength test, the shear force exerted on the web owing to the self-weight of the beam was omitted. The measured first shear cracking load was $V_{cr,\exp} = 1{,}200$ kN. It was assumed that the shear force was taken by the rectangular section of the web. Therefore, the average cracking shear strength of the UHPC beam

J. Bridge Eng., 2015, 20(8): B5014001

Downloaded from ascelibrary.org by Southeast University on 11/21/22. Copyright ASCE. For personal use only; all rights reserved.

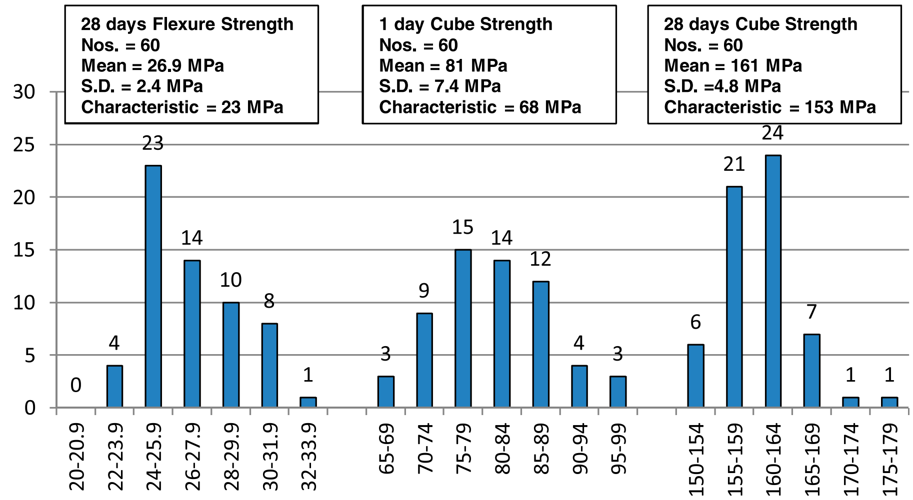

Fig. 7. Frequency distributions of compressive and flexural strengths of UHPC

Table 4. Design Actions, Design Resistances, and Experimental Results per Beam Equivalent

Stress resultant	Limit state	Design actions	Resistance (factored)	Ultimate (nonfactored)	Experimental results (Ikram QA Services 2011; Voo 2011)
Shear force (kN)	SLS	$V_{\text{ser}} = 537$	No provision	N/A	$V_{cr,\text{exp}} = 1{,}200$
	ULS	$V_{Ed} = 923$	$V_{Rd} = 1{,}056$	$V_{u,\text{theo}} = 1{,}405$	$V_{u,\text{exp}} > 1{,}403$[a]
Moment (kN · m)	SLS	$M_{\text{ser}} = 2{,}856$	$M_{cr} = 3{,}574$	N/A	$M_{cr,\text{exp}} = 3{,}830$[b] (joint open)
	ULS	$M_{Ed} = 4{,}848$	$M_{Rd} = 5{,}074$	$M_{u,\text{theo}} = 5{,}886$	$M_{u,\text{exp}} = 6{,}230$[b]

[a]Test stopped at that load step due to flexure.
[b]Includes moment due to self-weight of beam, $M_{G,\text{mid}} = 830$ kN · m.

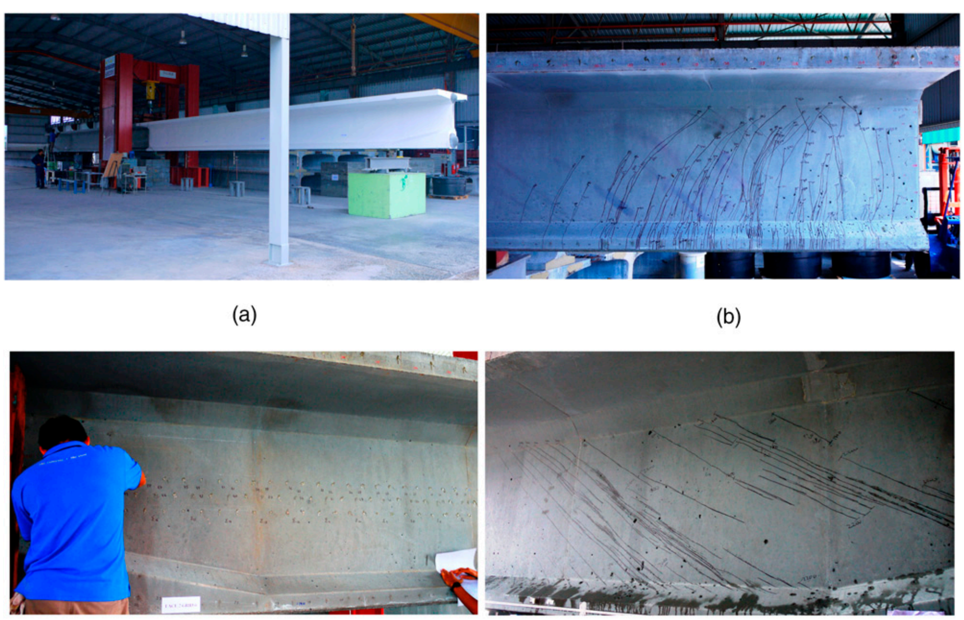

(a)

(b)

(c)

(d)

Fig. 8. (a) Flexure strength test setup; (b) crack pattern after test; (c) shear strength test setup; (d) crack pattern after test on the prototype UHPC beam (images by Yen Lei Voo)

Downloaded from ascelibrary.org by Southeast University on 11/21/22. Copyright ASCE. For personal use only; all rights reserved.

was approximately $\tau_{cr} = (1{,}200 \times 10^3)/(100 \times 1{,}325) = 9$ MPa. The shear strength test was stopped at the applied shear load of $V_{u,\mathrm{exp}} = 1{,}403$ kN because the UHPC beam was experiencing an applied moment of 5,290 kN · m, which was approximately 90% of theoretical ultimate moment capacity, $M_{u,\mathrm{theo}} = 5{,}886$ kN · m. In other words, the UHPC beam is unlikely to fail by critical diagonal web shear crack failure with a shear span to effective depth ratio of 3. Nevertheless, one can be sure that the UHPC beam has a shear strength beyond 10.6 MPa, and that it has ample shear resistance against the design shear force effects.

Construction

Construction Procedures

The construction sequence of the 90-m-long Sungai Nerok Bridge is similar to that of conventional RC bridges, except that some steps were skipped or simplified. The foundation work first was undertaken by piling contractors and, subsequently, the substructures were constructed (i.e., RC pile caps, RC abutments, and the intermediate piers). The RC end diaphragms were not constructed until the precast segmental UHPC beams were launched and seated on the abutments and pier crossheads. Each pair of 15-m-long beam segments, forming one girder, was transported from the factory using a 12-m-long, low-loader truck; the cargo weight was 28 t. Two 20-t capacity mobile cranes were used to unload the segments and the segments were assembled in an open space close to the bridge site. Once the shear-keyed segmental joints were aligned, strands were inserted into the ducts and posttensioning works were carried out by a specialist contractor. Prior to stressing of the beam, a layer of epoxy resin was applied to the dry joint; subsequently, the bottom and top tendons were stressed to 75% of the tendon guaranteed tensile strength (i.e., 19 strands $\times$ 260 kN $\times$ 0.75 = 3,705 kN for the bottom tendon and four strands $\times$ 260 kN $\times$ 0.75 = 780 kN for the top tendon).

Owing to the lightness of the UHPC beams (i.e., 29 t per beam, including strands and grouting), only one 200-t capacity mobile crane was used for the direct beam launching; the launching work took 5 days to complete. After the beams were positioned on their designated plinths, each member was connected to its adjacent beams to provide stability.

The next step was to lay the in situ UHPC between the starter steel bars, which were located at the beam top flanges to form the continuous deck. In total, the in situ UHPC needed to stitch the bridge girders together accounted for approximately 10% of the total superstructure weight. After completion of the stitching works, the end diaphragms were constructed using Grade 40 MPa concrete, which fully integrated the three spans.

A major step that was eliminated from that of conventional construction practice was the construction of a separate bridge deck. In this case, the bulk of the deck was integrated into the top flange of the girder and manufactured in the factory. Next, the RC parapets, wing walls, and approach slabs were constructed, and, lastly, the approaches and wearing course were laid.

Segmental Design Details

The concept of using segmental UHPC precast girder construction is to ensure ease of handling and transportation of the beam to site. In most rural areas, where access is poor and sourcing of larger capacity cranes is a major constraint, segmental construction allows the bridge designer to achieve longer spans with fewer, or without, central pier support located in the waterway. Besides, UHPC segmental construction improves constructability and minimizes temporary staging costs and construction time. In the case of the Sungai Nerok bridge, each beam consisted of one segmental joint at the midspan. The joint was an epoxied dry joint with four sets of 25-mm-deep shear keys. As the shear force is lowest at the beam midspan, the issue of shear capacity at the connection is not of critical concern.

Tendon Profile

One drawback of UHPC beam construction is that, owing to the thinness of the webs, providing inadequate cover to the corrugated tendon sheaths, the internal bonded tendon is usually straight in profile, with minimum rise at the anchorage zones. Therefore, some top prestress is needed to counterbalance the tensile stress generated by the high bottom tendon prestressing forces and also to ensure that the hog is not excessive. Fig. 6 shows the typical cross section of the UHPC beam that was used in the Sungai Nerok bridge; the web thickness was 100 mm, equal to that of the duct.

Cost Comparisons

The construction cost of the Sungai Nerok bridge was approximately RM4.0 million (US$1.25 million). This construction cost included the foundation/piling, substructure, superstructure, temporary works, and machinery and labor needed for the completion of the bridge. The cost did not include road works, slope protection, and relocation of existing utilities and services. In terms of a rate per square meter, the structural component cost for the bridge was US$906/m^2. This compares to the costs for conventional RC construction in Malaysia of approximately US$1,100 to $1,400/m^2, depending on the accessibility and difficulties in constructing the bridge. This project has shown the UHPC bridge is able to realize an immediate cost savings of at least 17%. Thus, it is evident that UHPC technology is cost-effective in bridge construction even before durability and longevity are considered.

Other Comments

This type of UHPC segmental integral beam-deck design is continually gaining acceptance as governmental bodies recognize its value and benefits. As shown in Table 1, in Malaysia, a total of 20 bridges have been completed to date using UHPC. Some of the advantages already have been realized, such as the significantly reduced construction time because in situ decking is not required. The reduction of beam weight also has made lifting and launching of the beam easier. Fewer temporary platform preparation and staging works are needed, and, in most cases, for a single-span bridge, only a single lifting crane is required to launch the beam.

The Public Works Department of Perak was the first to use the UHPC integral beam-deck system in the construction of a short-span single carriageway road bridge in remote, mountainous terrain of Malaysia. Construction of the Ulu Geroh bridge commenced in November 2011 and was completed in January 2012. This bridge was designed to withstand 30 U of HB loading (equivalent to 132 and 156 t per lane at SLS and ULS, respectively) and HA + KEL loading, as per BD 37/01. The bridge has a single-span length of 25 m, a 3.5-m full carriageway width, and was constructed using two segmental UHPC T-girders that resemble those in Fig. 6 (except that the top flange was 1.5 m wide).

The major obstacle in this project was the poor access road to the bridge site. The largest vehicles able to access the site were the 20-t all-terrain crane and 10-wheel trucks (i.e., double axle), which come with a tray length not exceeding 6 m. Given such constraints, the conventional precast RC beams were ruled out immediately because the self-weight of a 25-m-long conventional precast RC beam exceeds the carrying capacity of the mobile cranes. The other

J. Bridge Eng., 2015, 20(8): B5014001

Downloaded from ascelibrary.org by Southeast University on 11/21/22. Copyright ASCE. For personal use only; all rights reserved.

possible option was using a steel bridge, where the girder weight is not a major issue. However, the authorities rejected this option because a maintenance-free bridge was required. In addition, the design criteria specified that there must be no central pier in the waterway. With these limitations, the UHPC bridge system proved to be the best solution as a single UHPC T-beam weighs only 25 t and the girder has remarkable durability. Unlike the Sungai Nerok bridge, where each UHPC beam was formed from two 15-m-long precast segments, the Ulu Geroh bridge girders were composed of five individual segments per beam supplied in segmental lengths of 5 m each. Each segment was transported to site using a smaller truck. This approach further demonstrates that the UHPC bridges have the flexibility to be customized to suit each bridge site condition in terms of its feasibility and constructability.

Conclusions

In this paper, the current state of practice was presented in the development of UHPC segmental bridge construction in Malaysia. Since 2006, and in collaboration with the Malaysia Works Ministry, DT has pioneered research in the optimal uses of UHPC in bridge construction through its Sustainable Bridge Construction Initiative. After several years of research and development work in design and building of UHPC bridges in rural regions (where sourcing of material, site access, and construction methods can be major challenges when using conventional construction methods) and in the cities, 20 UHPC segmental bridges have been constructed and are open for service. Another six bridges are to be completed before the end of 2014.

A case study was presented for the three-span, 90-m-long, Sungai Nerok bridge that was constructed in 2013 in Perak state, Malaysia. The case study demonstrated various design and construction aspects, such as quality control, constructability, and of how UHPC helped to make the bridge more affordable, sustainable, easier to construct, and economical. From projects such as these, and others being developed around the world, it is clear that UHPC has an important role to play in construction technologies in developed and developing countries alike.

References

Behloul, M., and Lee, K. C. (2003). "Ductal® Seonyu footbridge." *Struct. Concr.*, 4(4), 195–201.

Blais, P. Y., and Couture, M. (1999). "Precast, prestressed pedestrian bridge—World's first reactive powder concrete structure." *PCI J.*, 44(5), 60–71.

Buyukozturk, O., Bakhoum, M. M., and Beattie, S. M. (1990). "Shear behavior of joints in precast concrete segmental bridges." *J. Struct. Eng.*, 10.1061/(ASCE)0733-9445(1990)116:12(3380), 3380–3401.

Foster, S. J. (2009). "The application of steel-fibres as concrete reinforcement in Australia: From material to structure." *Mater. Struct.*, 42(9), 1209–1220.

Freytag, B., Heinzle, G., Reichel, M., and Sparowitz, L. (2012). "WILD-bridge scientific preparation for smooth realisation." *Proc., 3rd Int. Symp. on UHPC and Nanotechnology for High Performance Construction Materials*, M. Schmidt, E. Fehling, C. Glotzbach, S. Fröhlich, and S. Piotrowski, eds., Kassel University Press, Kassel, Germany, 881–888.

Graybeal, B. (2011). "UHPC in US highway infrastructure." Chapter 15, *Designing and building with UHPFRC: State of the art and development*, F. Toutlemonde and J. Resplendino, eds., ISTE, London, 221–234.

Highways Agency. (2001). "Loads for highway bridges." *BD 37/01*, Dept. for Transport, London.

Ikram QA Services. (2011). "Flexure and shear strength test of T-bridge girder (TBG1325)." *Test Rep. FS6A01/454/11*, Material Testing Laboratory, Selangor, Malaysia.

Japan Society of Civil Engineers (JSCE). (2006). "Recommendations for design and construction of ultra high strength fiber reinforced concrete structures (draft)." *JSCE Guidelines for concrete No. 9*, Tokyo.

Kaptijn, N., and Blom, J. (2004). "A new bridge deck for the Kaag bridges—The first CRC (compact reinforced composite) application in civil infrastructure." *Proc., Int. Symp. on Ultra High Performance Concrete*, M. Schmidt, E. Fehling, and C. Geisenhanslüke, eds., Kassel University Press, Kassel, Germany, 49–57.

Kim, B.-S., Kim, S., Kim, Y.-J., Park, S. Y., Koh, K.-T., and Joh, C. (2012). "R&D activities and application of ultra high performance concrete to cable-stayed bridges." *Proc., 3rd Int. Symp. on UHPC and Nanotechnology for High Performance Construction Materials*, M. Schmidt, E. Fehling, C. Glotzbach, S. Fröhlich, and S. Piotrowski, eds., Kassel University Press, Kassel, Germany, 865–872.

Lachemi, M., Bastien, J., Adeline, R., Ballivy, G., and Aïtchin, P. C. (1998). "Monitoring of the world's first reactive powder concrete bridge." *Proc., 5th Int. Conf. on Short and Medium Span Bridges* (CD-ROM), Canadian Society for Civil Engineering, Calgary, Canada.

Li, G., Yang, D., and Lei, Y. (2013a). "Combined shear and bending behavior of joints in precast concrete segmental beams with external tendons." *J. Bridge Eng.*, 10.1061/(ASCE)BE.1943-5592.0000453, 1042–1052.

Li, G., Zhang, C., and Niu, C. (2013b). "Experimental study on shear behavior in negative moment regions of segmental externally prestressed concrete continuous beams." *J. Bridge Eng.*, 10.1061/(ASCE)BE.1943-5592.0000351, 328–338.

Musha, H., Ohkuma, H., and Kitamura, T. (2013). "Innovative UFC structures in Japan." *Proc., RILEM-fib-AFGC Int. Symp. on Ultra High Performance Fibre-Reinforced Concrete (UHPFRC)*, F. Toutlemonde and J. Resplendino, eds., RILEM, Bagneux, France, 17–26.

Ng, T. S., Voo, Y. L., and Foster, S. J. (2012). "Sustainability with ultra-high performance and geopolymer concrete construction." Chapter 5, *Innovative materials and techniques in concrete construction*, M. N. Fardis, ed., Springer, Dordrecht, Netherlands, 81–100.

Rebentrost, M., and Wight, G. (2011). "Perspective on UHPCs from a specialist construction company." Chapter 13, *Designing and building with UHPFRC: State of the art and development*, F. Toutlemonde and J. Resplendino, eds., ISTE, London, 189–206.

Resplendino, J. (2008). "Ultra-high performance concretes—Recent realizations and research programs on UHPFRC bridges in France." *Proc., 2nd Int. Symp. on Ultra High Performance Concrete*, E. Fehling, M. Schmidt, and S. Stürwald, eds., Kassel University Press, Kassel, Germany, 31–43.

Ricciotti, R. (2002). "The Footbridge of Peace, Seoul, South Korea." *Concrete (Lond.)*, 36(10), 11–13.

RILEM. (2002). "Recommendations of RILEM TC 162-TDF: Test and design methods for steel fibre reinforced concrete: Bending test." *Mater. Struct.*, 35(253), 579–582.

Saibabu, S., Srinivas, V., Sasmal, S., Lakshmanan, N., and Iyer, N. R. (2013). "Performance evaluation of dry and epoxy jointed segmental prestressed box girders under monotonic and cyclic loading." *Construct. Build. Mater.*, 38(Jan), 931–940.

Šajna, A., Denarié, E., and Bras, V. (2012). "Assessment of a UHPFRC based bridge rehabilitation in Slovenia, two years after application." *Proc., 3rd Int. Symp. on UHPC and Nanotechnology for High Performance Construction Materials*, M. Schmidt, E. Fehling, C. Glotzbach, S. Fröhlich, and S. Piotrowski, eds., Kassel University Press, Kassel, Germany, 937–944.

Schmidt, M. (2012). "Sustainable building with ultra-high-performance concrete (UHPC)—Coordinated research program in Germany." *Proc., 3rd Int. Symp. on UHPC and Nanotechnology for High Performance Construction Materials*, M. Schmidt, E. Fehling, C. Glotzbach, S. Fröhlich, and S. Piotrowski, eds., Kassel University Press, Kassel, Germany, 17–25.

Tanaka, Y., Maekawa, K., Kameyama, Y., Ohtake, A., Musha, H., and Watanabe, N. (2011). "The innovation and application of UHPFRC bridges in Japan." Chapter 12, *Designing and building with UHPFRC: State of the art and development*, F. Toutlemonde and J. Resplendino, eds., ISTE, London, 149–187.

Toutlemonde, F., and Resplendino, J. (2011). *Designing and building with UHPFRC: State of the art and development*, ISTE, London.

Downloaded from ascelibrary.org by Southeast University on 11/21/22. Copyright ASCE. For personal use only; all rights reserved.

Voo, Y. L. (2011). "Experimental study on structural behaviour of ultra-high performance ductile concrete post-tensioned T-bridge girder (DURA® TBG1325)." *Technical Rep. No. TR-0007*, Dura Technology, Chemor, Perak, Malaysia.

Voo, Y. L., Augustin, P. C., and Thamboe, T. A. J. (2011). "Construction and design of a 50M single span UHP ductile concrete composite road bridge." *Structural Engineer*, 89(15–16), 24–31.

Voo, Y. L., and Foster, S. J. (2010). "Characteristics of ultra-high performance 'ductile' concrete and its impact on sustainable construction." *IES J. Part A: Civ. Struct. Eng.*, 3(3), 168–187.

Voo, Y. L., Foster, S. J., and Gilbert, R. I. (2006). "Shear strength of fiber reinforced reactive powder concrete prestressed girders without stirrups." *J. Adv. Concr. Technol.*, 4(1), 123–132.

Voo, Y. L., Poon, W. K., and Foster, S. J. (2010). "Shear strength of steel fiber-reinforced ultrahigh-performance concrete beams without stirrups." *J. Struct. Eng.*, 10.1061/(ASCE)ST.1943-541X.0000234, 1393–1400.

Zhou, X., Mickleborough, N., and Li, Z. (2005). "Shear strength of joints in precast concrete segmental bridges." *ACI Struct. J.*, 102(1), 3–11.

Downloaded from ascelibrary.org by Southeast University on 11/21/22. Copyright ASCE. For personal use only; all rights reserved.